

Supporting Information

Multi-controlled Ternary Emission of Platinum (II) Switches as Visually Optical Sensor for Enzyme and pH Detection

Zhu Shu,^{1,2} Xin Lei,¹ Qingguo Zeng,¹ Yeye Ai,^{1*} XinYi Chen,² Yanglin Lv,² Yunchu Shao,² Guohua Ji,³ Tingjing Sun,¹ Guanjun Xiao,^{1,4} Yongguang Li^{1*}

1 College of Material, Chemistry and Chemical Engineering, Key Laboratory of Organosilicon Chemistry and Material Technology Ministry of Education, Hangzhou Normal University, Hangzhou 311121, China

2 Kharkiv Institute, Hangzhou Normal University, Hangzhou 311121, China

3 Hangzhou Polytechnic, Hangzhou 311402, China

4 State Key Laboratory of Superhard Materials, College of Physics, Jilin University, Changchun 130012, P. R. China

E-mail: aiyeeye@hznu.edu.cn; yongguangli@hznu.edu.cn

Table of Contents

1. Material and Methods	3
1.1 Chemicals.....	3
1.2 Physical Measurements and Instrumentations	3
2. Synthetic Methods and Characterization	4
Scheme S1. Synthetic routes of complex 1	4
2.1 Synthesis of compound 1-1	4
2.2 Synthesis of compound 1-3	5
2.3 Synthesis of complex 1	5
3. Supporting Figures	7
Figure S1. Concentration-dependent UV-Vis absorption and emission spectra of 1	7
Figure S2. The phosphorescent lifetime of 1	7
Figure S3. Lambert-Beer plot of 1 in DMF solution from 0.2 mM to 2.0 mM.	8
Figure S4. Excitation spectra of 1 in DMF solution.	8
Figure S5. Emission spectra of 1 in the aqueous solution at various pH values.....	9
Figure S6. Excitation spectra of 1 in the aqueous solution upon addition of KOH.....	9
Figure S7. DLS studies of 1 , 1 +KOH and 1 +CH ₃ COOH in aqueous solution.....	10
Figure S8. Emission intensity changes of 1 at 520 nm as a function of acid-titrated pH.	10
Figure S9. Emission intensity changes of 1 at 800 nm as a function of base-titrated pH.....	11
Figure S10. Partial ¹ H NMR spectra of 1 (DMSO- <i>d</i> ₆), 1 (D ₂ O), and 1 -ATP (D ₂ O).....	11
Figure S11. UV-Vis absorption spectra of 1 and 1 -ALP in Tris-HCl and MgCl ₂ buffer solution.	12
Figure S12. ESI-MS(+) spectrum of AMP in solution of 1 -ATP-ALP.	12
Figure S13. ESI-MS(-) spectrum of AMP in solution of 1 -ATP-ALP.	13
Figure S14. Structures of the anionic phosphates used in this work.....	13
Figure S15. UV-Vis absorption and emission spectra of 1 -ADP.	14
Figure S16. DLS studies of 1 with the increased concentration of ADP.....	14
Figure S17. UV-Vis absorption and emission spectra of 1 -AMP.....	15
Figure S18. DLS studies of 1 with the increased concentration of AMP.	15
Figure S19. UV-Vis absorption and emission spectra of 1 -UTP.	16
Figure S20. DLS studies of 1 with the increased concentration of UTP.	16
Figure S21. UV-Vis absorption and emission spectra of 1 -GTP.....	17
Figure S22. DLS studies of 1 with the increased concentration of GTP.	17
Figure S23. ¹ H NMR spectrum of 1-1 in CDCl ₃	18
Figure S24. ¹³ C NMR spectrum of 1-1 in CDCl ₃	18
Figure S25. ¹ H NMR spectrum of 1-3 in DMSO- <i>d</i> ₆	19
Figure S26. ¹³ C NMR spectrum of 1-3 in DMSO- <i>d</i> ₆	19
Figure S27. ¹⁹ F NMR spectrum of 1-3 in DMSO- <i>d</i> ₆	20
Figure S28. ¹ H NMR spectrum of 1 in DMSO- <i>d</i> ₆	20
Figure S29. ¹³ C NMR spectrum of 1 in DMSO- <i>d</i> ₆	21
Figure S30. ¹⁹ F NMR spectrum of 1 in DMSO- <i>d</i> ₆	21
Figure S31. Infrared spectrum of 1	22
4. References	22

1. Material and Methods

1.1 Chemicals

All chemicals and solvents were used without further purification. 2-Bromonicotinic acid (95 %, Aladdin), tert-butyl(6-aminohexyl) carbamate (98 %, Aladdin), 1-ethyl-3-(3-dimethylaminopropyl)carbodiimide hydrochloride (EDC·HCl, 98 %, Aladdin), 1-hydroxybenzo-trizole (HOBT, 99 %, Energy Chemical), 4-dimethylamino-pyridine (DMAP, 99 %, Alfa Aesar), tetrakis(triphenylphosphine) palladium (99.8 %, Alfa Aesar), potassium carbonate (99 %, Innochem), potassium tetrachloroplatinate(II) (K_2PtCl_4 , 99 %, Energy Chemical), guanosine-5'-triphosphoric acid disodium salt (GTP, 90 %, Energy Chemical), uridine 5'-triphosphate trisodium salt hydrate (UTP, 98 %, Energy Chemical), adenosine 5'-diphosphate (ADP, 97 %, Energy Chemical), adenosine 5'-triphosphate (ATP, 98 %, Energy Chemical), adenosine 5'-monophosphate (AMP, 98 %, Energy Chemical) were used as received.

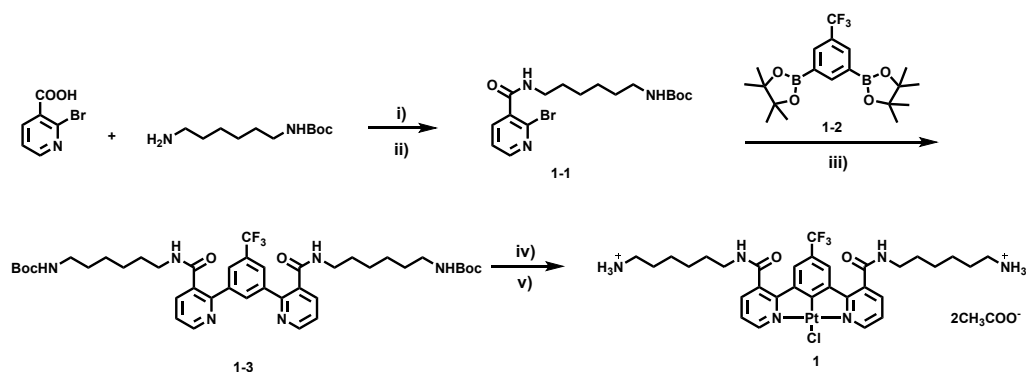
1.2 Physical Measurements and Instrumentations

1H NMR, ^{13}C NMR, ^{19}F NMR, and temperature-dependent 1H NMR spectra were recorded on a Bruker DPX 500 FT-NMR spectrometer (500 MHz). Elemental analysis of the complex was performed on a Vario EL III elemental analyzer. High-resolution mass spectra were obtained by electrospray ionization (ESI) on a quadrupole-orbitrap mass spectrometer (6530 Q-TOF LC/MS, Agilent). Electronic absorption spectra were recorded using a Shimadzu UV-2600 spectrophotometer. The photoluminescence spectra were measured on PerkinElmer FL 6500 and Edinburgh Instruments FLS980 fluorescence spectrophotometers. Circular dichroism spectra were recorded using a Chirascan-plus V100 CD spectropolarimeter. Transmission electron micrographs (TEM) were recorded on an HT-7700 electron microscope operated at an acceleration voltage of 70 kV. Drop casting solutions on the carbon-coated copper grids prepared the samples for TEM. Dynamic light scattering (DLS) experiments were conducted on a Brookhaven BI-9000AT instrument. Infrared spectra were collected on a Bruker

VERTEX 70v. The emission quantum yields were measured on a Hamamatsu C13534 absolute PL quantum yield measurement system.

2. Synthetic Methods and Characterization

2,2'-(5-(Trifluoromethyl)-1,3-phenylene)bis(4,4,5,5-tetramethyl-1,3,2-dioxaborolane) (Complex **1-2**) in Schemes S1 was synthesized according to the reported literature.^[1]



Scheme S1. Synthetic routes of complex **1**. i) EDC·HCl, HOBT, DMAP; ii) DMF/CH₂Cl₂; iii) Pd(PPh₃)₄, K₂CO₃, H₂O/DME; iv) K₂PtCl₄; v) CH₃COOH.

2.1 Synthesis of compound 1-1

To a DMF (30 mL) solution of 2-bromonicotinic acid (500 mg, 2.48 mmol) and tert-butyl (6-aminohexyl) carbamate (642 mg, 2.97 mmol) in a 100 mL flask were added EDC·HCl (710 mg, 3.72 mmol), HOBT, (401 mg, 2.97 mmol), and DMAP (30 mg, 0.25 mmol). The mixture was stirred overnight at room temperature. To the reaction mixtures H₂O (300 mL) was added and extracted with CH₂Cl₂ (150 mL) for three times. The combined organic phase was washed with H₂O (100 mL) for three times and dried over anhydrous MgSO₄. After filtration and removal of the solvent under reduced pressure afforded the crude product, which was purified by flash column chromatography (ethyl acetate /CH₂Cl₂, 1:2 v/v) to give compound **1-1** (714.2 mg, 72 %). ¹H NMR (500 MHz, CDCl₃, relative to Me₄Si, δ / ppm): 8.41 (dd, J = 4.7, 2.0 Hz, 1H), 7.89 (dd, J = 7.6, 1.9 Hz, 1H), 7.34 (dd, J = 7.6, 4.8 Hz, 1H), 6.41 (s, 1H), 4.54 (s, 1H), 3.46 (dd, J = 13.0, 6.9 Hz, 2H), 3.12 (d, J = 6.2 Hz, 2H), 1.67–1.63 (m, 2H), 1.50–1.35 (m, 16H). ¹³C NMR (126 MHz, CDCl₃, δ / ppm): 165.70, 156.09, 150.99, 138.51,

122.84, 40.15, 39.92, 30.04, 29.10, 28.41, 26.27, 26.00.

2.2 Synthesis of compound 1-3

A mixture of **1-1** (400 mg, 1 mmol), **1-2** (190 mg, 0.47 mmol), K₂CO₃ (519 mg, 3.76 mmol), and Pd(PPh₃)₄ (55 mg, 0.047 mmol) in DME/H₂O (1:1 v/v, 100 mL) was refluxed for 24 h under nitrogen atmosphere. Upon completion of the reaction, the solvent was extracted with CH₂Cl₂/H₂O. The organic phase was washed with brine and dried over anhydrous MgSO₄. After filtration and Removal of the solvent under reduced pressure, the crude product was purified by column chromatography (DCM/methanol, 20:1 v/v as the eluent) to give compound **1-3** (147 mg, 40 %). ¹H NMR (500 MHz, DMSO-*d*₆, relative to Me₄Si, δ / ppm): 8.75 (dd, *J* = 4.8, 1.6 Hz, 2H), 8.52 (t, *J* = 5.6 Hz, 2H), 8.31 (s, 1H), 7.96 (s, 2H), 7.87 (dd, *J* = 7.7, 1.6 Hz, 2H), 7.50 (dd, *J* = 7.7, 4.8 Hz, 2H), 6.72 (t, *J* = 5.4 Hz, 2H), 3.10–3.06 (m, 4H), 2.87–2.83 (m, 4H), 1.36 (s, 18H), 1.29 (d, *J* = 6.5 Hz, 8H), 1.10 (d, *J* = 3.1 Hz, 8H). ¹³C NMR (126 MHz, DMSO-*d*₆, δ / ppm): 168.09, 156.04, 153.41, 150.35, 140.72, 136.82, 133.33, 123.18, 77.73, 29.83, 28.85, 28.73, 26.55, 26.33.

2.3 Synthesis of complex 1

1-3 (147 mg, 0.188 mmol) and K₂PtCl₄ (94 mg, 0.23 mmol) were added into glacial acetic acid and the mixtures were refluxed for 3 days. After cooling to room temperature, the product was obtained upon slowly precipitated with ethyl acetate in batches, which was subsequently recrystallized from methanol and ethyl acetate (77 mg, 50.1%). ¹H NMR (500 MHz, DMSO-*d*₆, relative to Me₄Si, δ / ppm): 9.41 (dd, *J* = 5.7, 1.6 Hz, 2H), 9.15 (t, *J* = 5.5 Hz, 2H), 8.22 (dd, *J* = 7.8, 1.6 Hz, 2H), 7.47-7.77 (m, 10H), 3.32-3.36 (m, 4H, mixed with H₂O peak), 2.73-2.78 (m, 4H), 1.90 (s, 1.18H), 1.77 (s, 4.75), 1.51-1.61 (m, 8H), 1.28-1.39 (m, 8H). ¹³C NMR (126 MHz, DMSO-*d*₆, δ / ppm): 169.41, 165.90, 161.02, 152.42, 140.52, 140.07, 133.77, 125.50, 123.66, 29.49, 28.79, 27.55, 26.46, 26.00, 25.59, 23.05. MS (ESI): *m/z*: [1-H]⁺: at 814.5765. Elemental analysis calcd (%) for C₃₅H₄₆ClF₃N₆O₆Pt•H₂O: C 44.14, H 5.08, N 8.82; found: C 44.07, H 5.16, N 8.90.

3. Supporting Figures

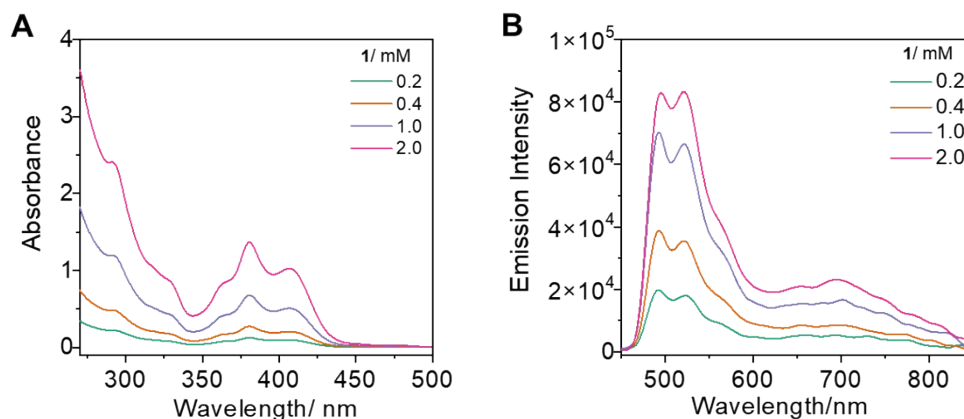


Figure S1. Concentration-dependent (A) UV-Vis absorption and (B) emission spectra of **1** in DMF solution from 0.2 mM to 2 mM. $\lambda_{\text{ex}} = 400$ nm.

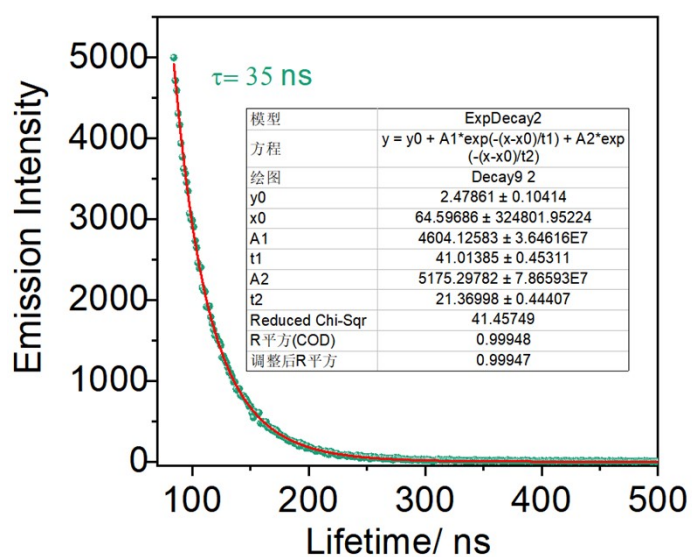


Figure S2. The phosphorescent lifetime of **1** (0.02 mM) in DMF solution at the emission wavelength of 489 nm.

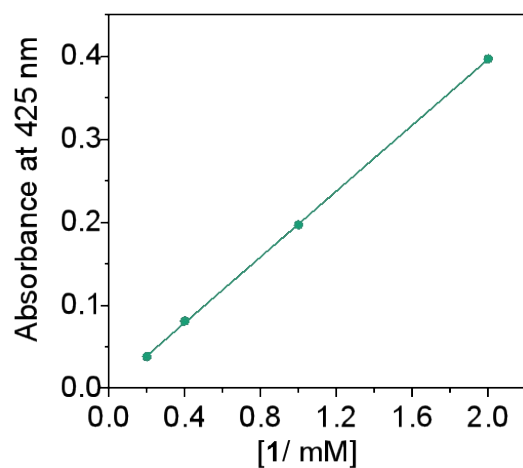


Figure S3. Lambert-Beer plot of **1** in DMF solution from 0.2 mM to 2.0 mM.

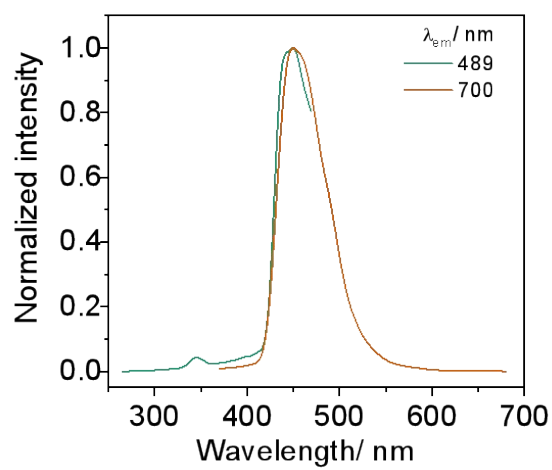


Figure S4. Excitation spectra of **1** (2.0 mM) in DMF solution.

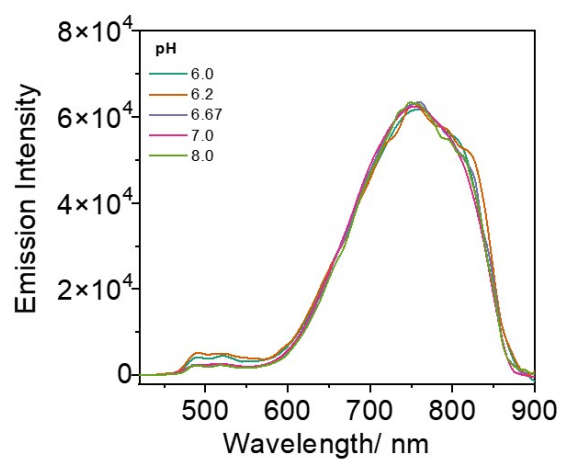


Figure S5. Emission spectra of **1** (0.2 mM) in the aqueous solution at various pH values.

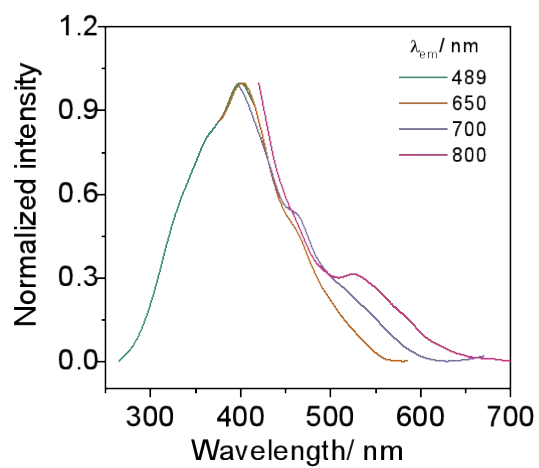


Figure S6. Excitation spectra of **1** (0.2 mM) in the aqueous solution upon addition of KOH (0.05 M, 10 μ L).

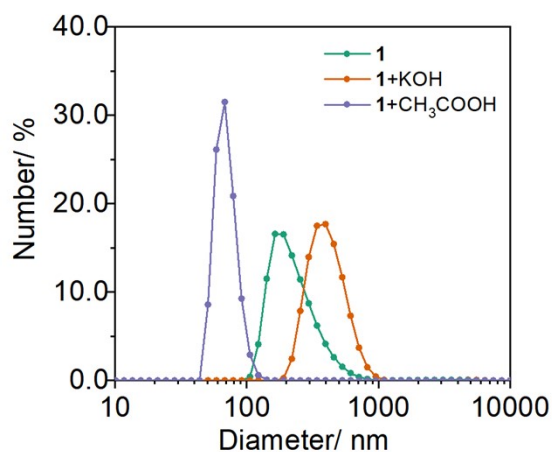


Figure S7. DLS studies of **1** (0.2 mM), **1**+KOH (pH=11) and **1**+CH₃COOH (pH=2.32) in aqueous solution.

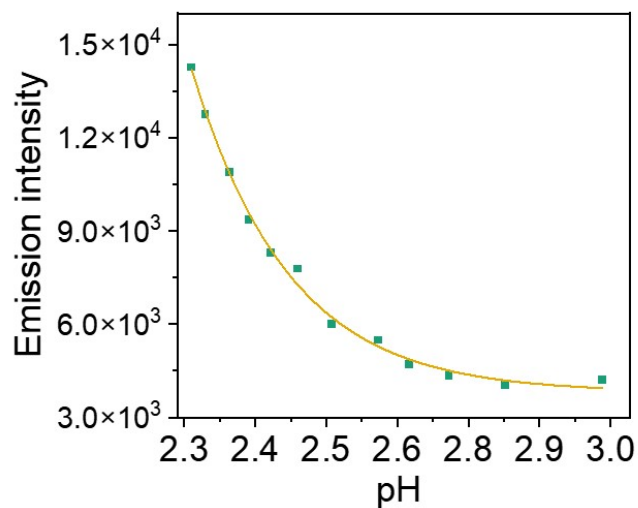


Figure S8. Emission intensity changes of **1** at 520 nm as a function of acid-titrated pH.

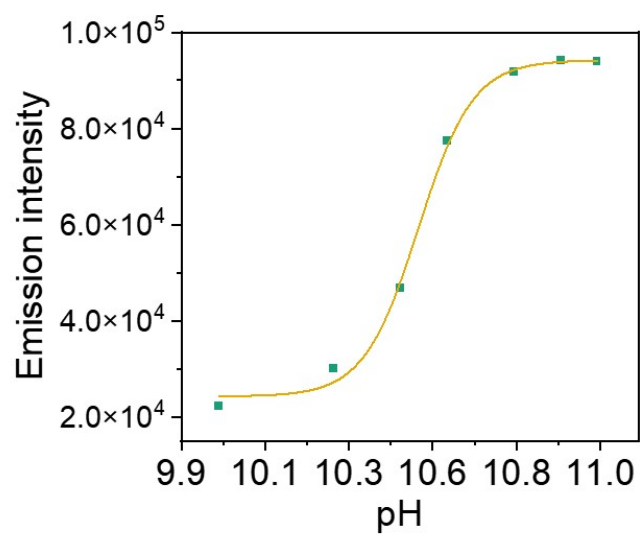


Figure S9. Emission intensity changes of **1** at 800 nm as a function of base-titrated pH.

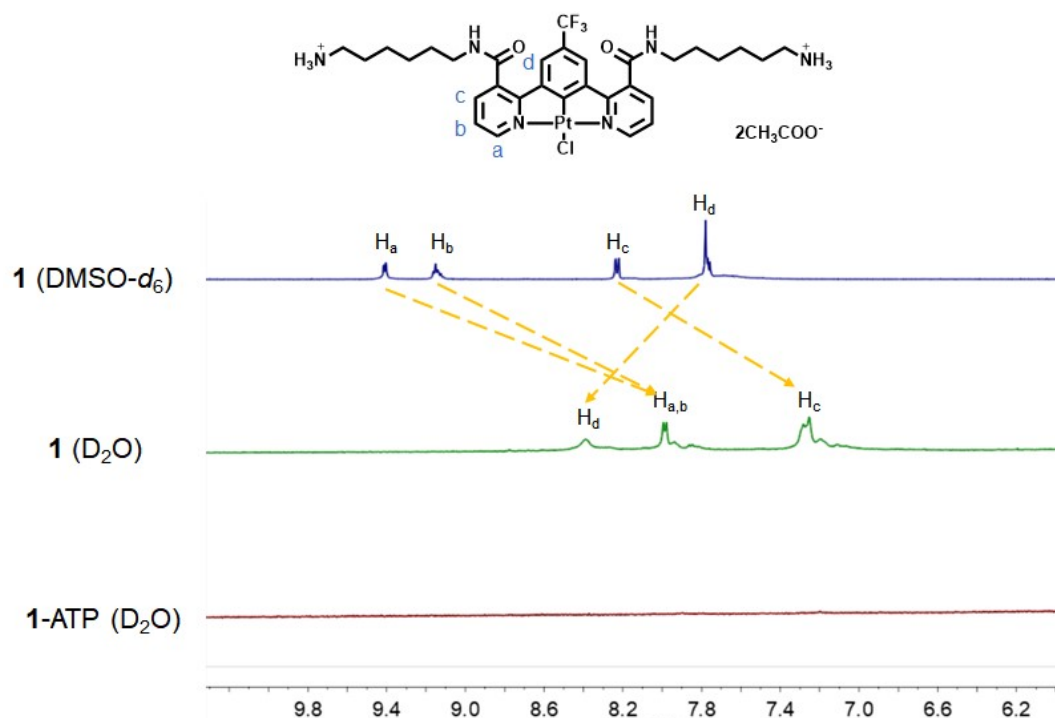


Figure S10. Partial ^1H NMR spectra of **1** (0.2 mM in $\text{DMSO-}d_6$), **1** (0.2 mM in D_2O), and **1-ATP** (0.2 and 0.015 mM of **1** and ATP, respectively, in D_2O).

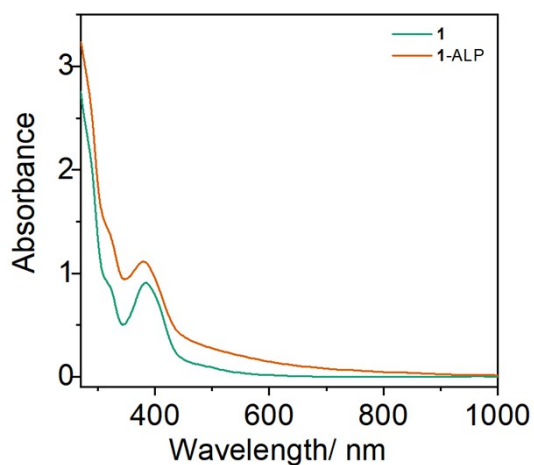


Figure S11. UV-Vis absorption spectra of **1** (0.2 mM) and **1-ALP** (0.2 mM) in Tris-HCl (50 mM) and MgCl_2 (20 mM) buffer solution.

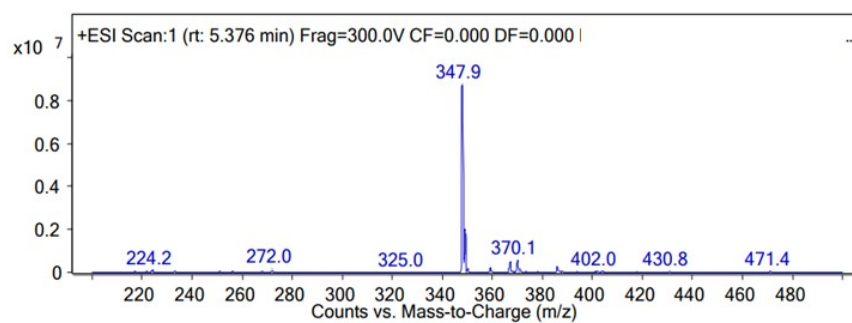
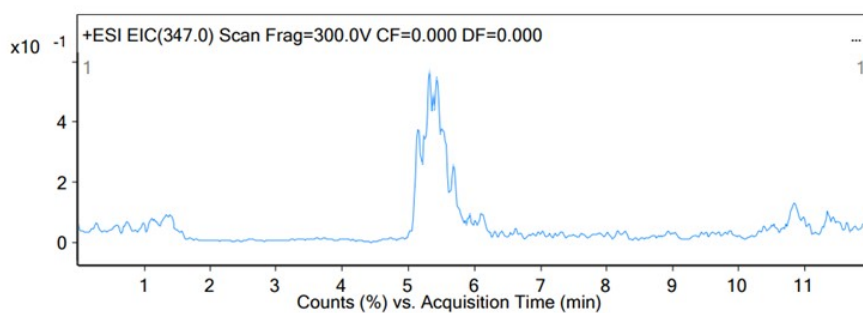


Figure S12. ESI-MS(+) spectrum of AMP in solution of **1**-ATP-ALP.

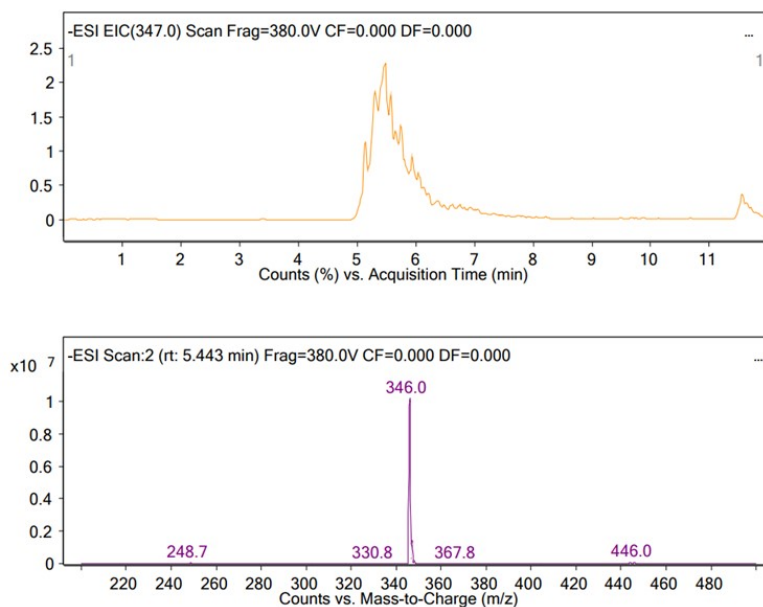


Figure S13. ESI-MS(-) spectrum of AMP in solution of **1**-ATP-ALP.

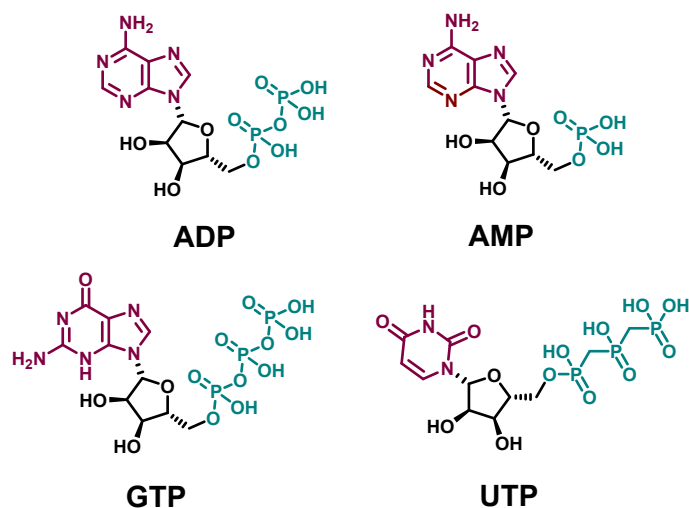


Figure S14. Structures of the anionic phosphates used in this work.

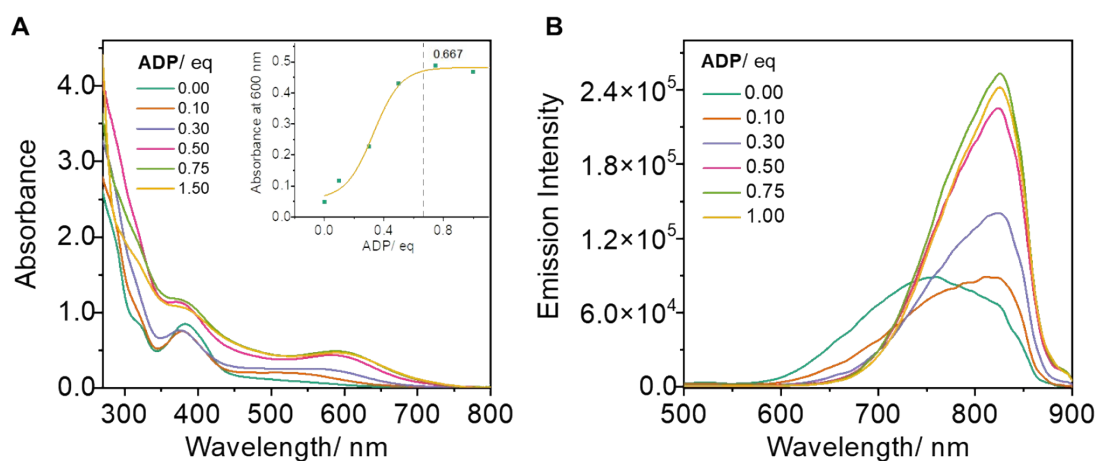


Figure S15. (A) UV-Vis absorption and (B) emission spectra of **1** (0.2 mM) in Tris-HCl (50 mM) buffer solution upon gradual addition of ADP (0-1.0 eq). (Insets: the absorption intensity changes at $\lambda = 600$ nm with the increased concentration of ADP.)

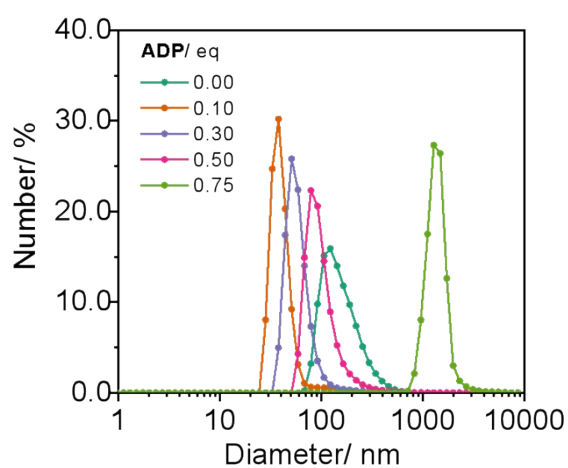


Figure S16. DLS studies of **1** (0.2 mM) with the increased concentration of ADP.

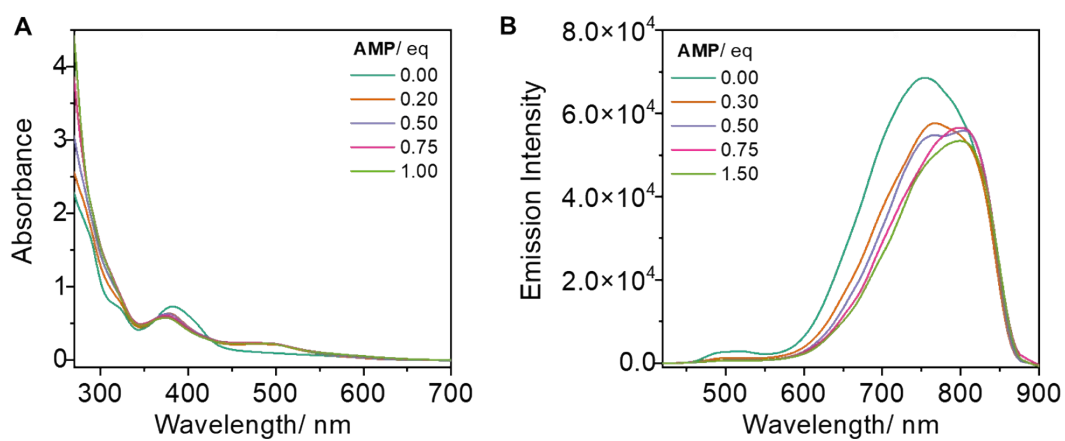


Figure S17. (A) UV-Vis absorption and (B) emission spectra of **1** (0.2 mM) in Tris-HCl (50 mM) buffer solution upon gradual addition of AMP (0-1.0 eq).

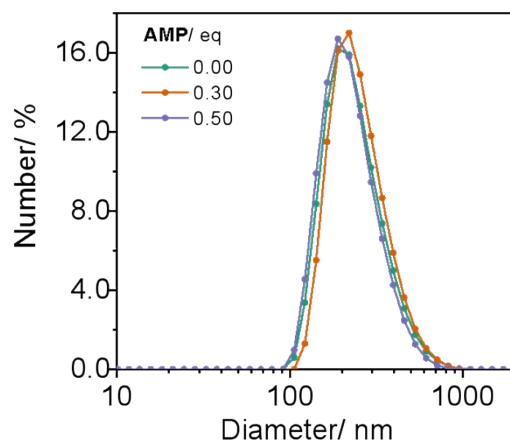


Figure S18. DLS studies of **1** (0.2 mM) with the increased concentration of AMP.

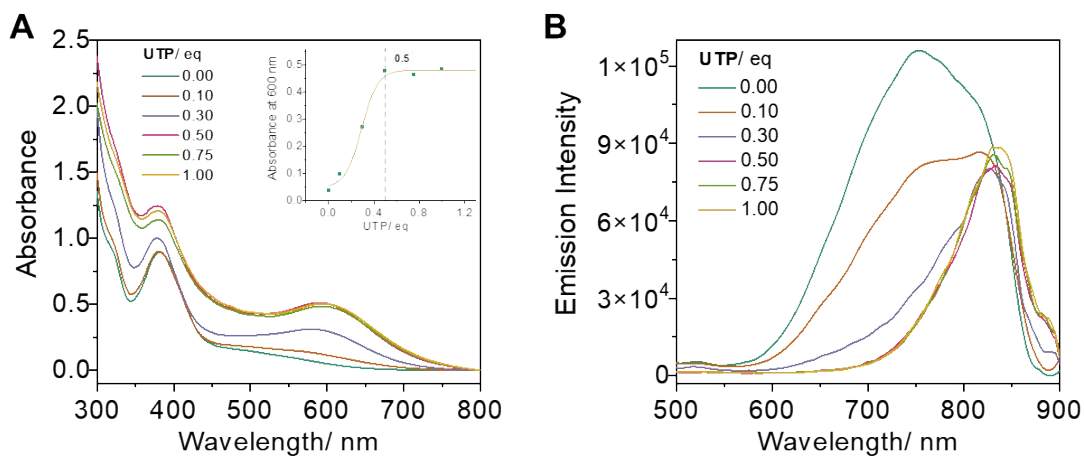


Figure S19. (A) UV-Vis absorption and (B) emission spectra of **1** (0.2 mM) in Tris-HCl (50 mM) buffer solution upon gradual addition of UTP (0-1.0 eq). (Insets: the absorption intensity changes at $\lambda = 600$ nm with the increased concentration of UTP.)

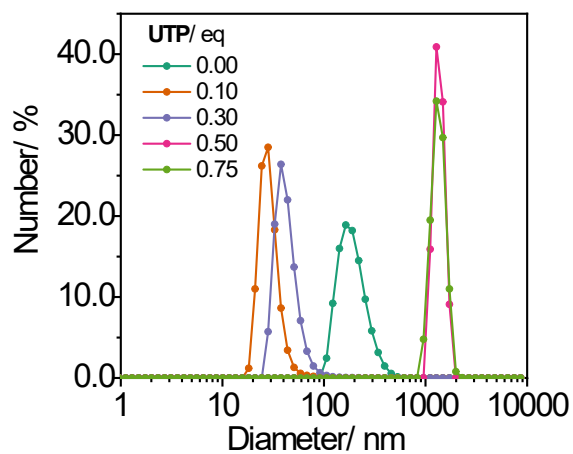


Figure S20. DLS studies of **1** (0.2 mM) with the increased concentration of UTP.

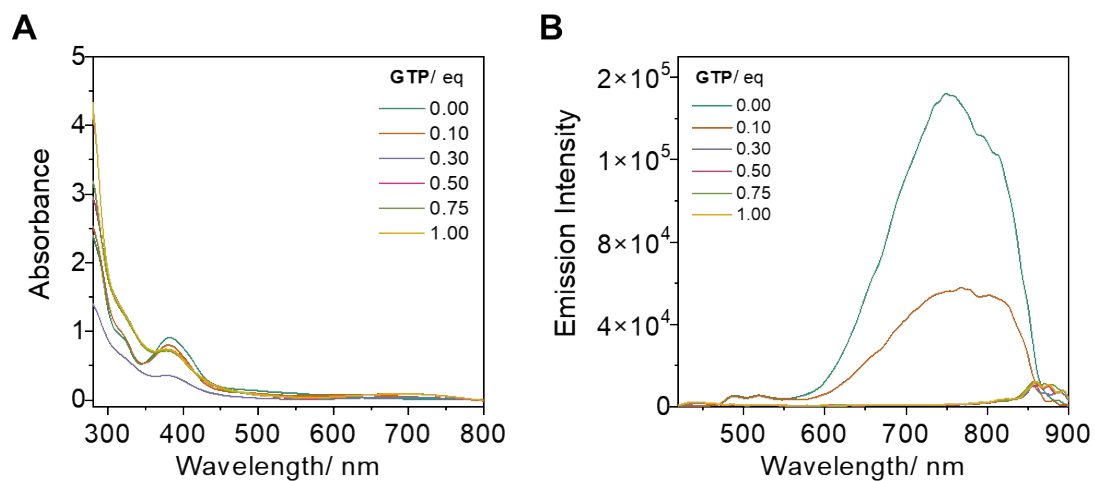


Figure S21. (A) UV-Vis absorption and (B) emission spectra of **1** (0.2 mM) in Tris-HCl (50 mM) buffer solution upon gradual addition of GTP (0-1.0 eq).

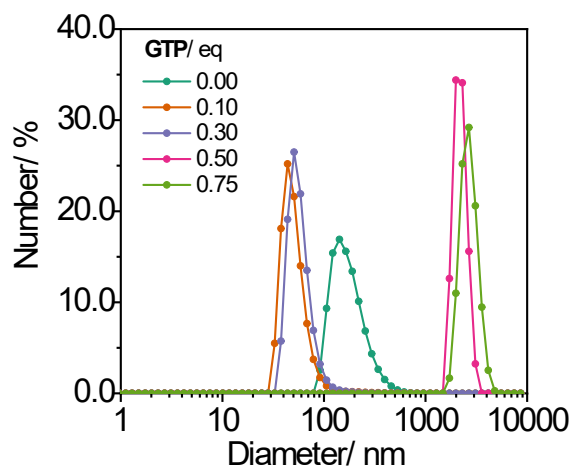


Figure S22. DLS studies of **1** (0.2 mM) with the increased concentration of GTP.

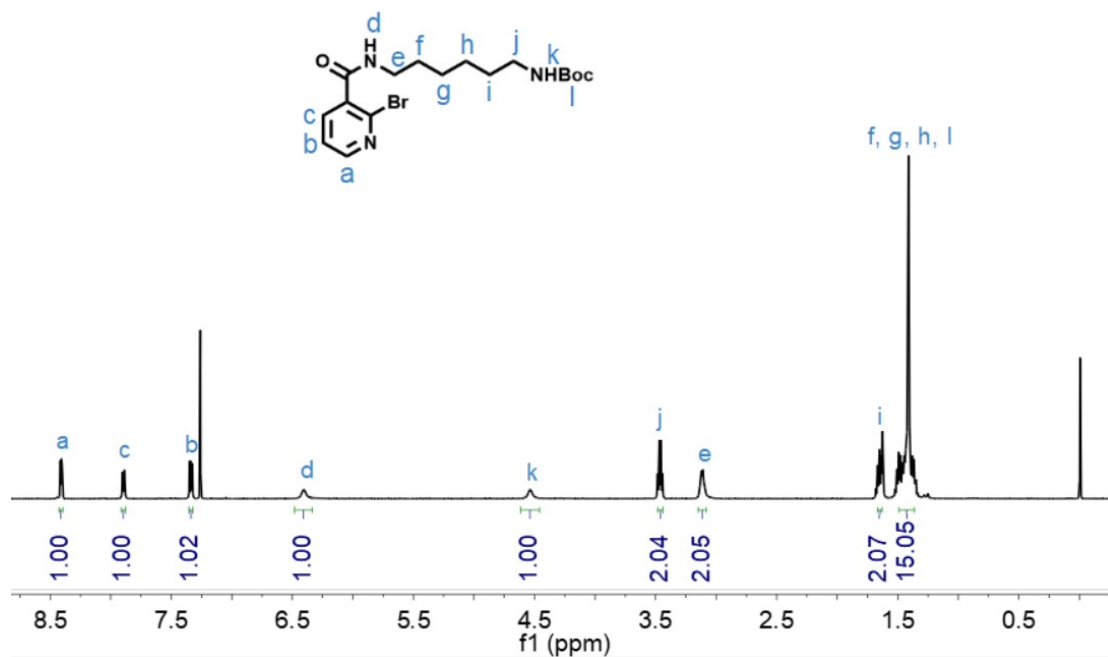


Figure S23. ¹H NMR spectrum of **1-1** in CDCl₃.

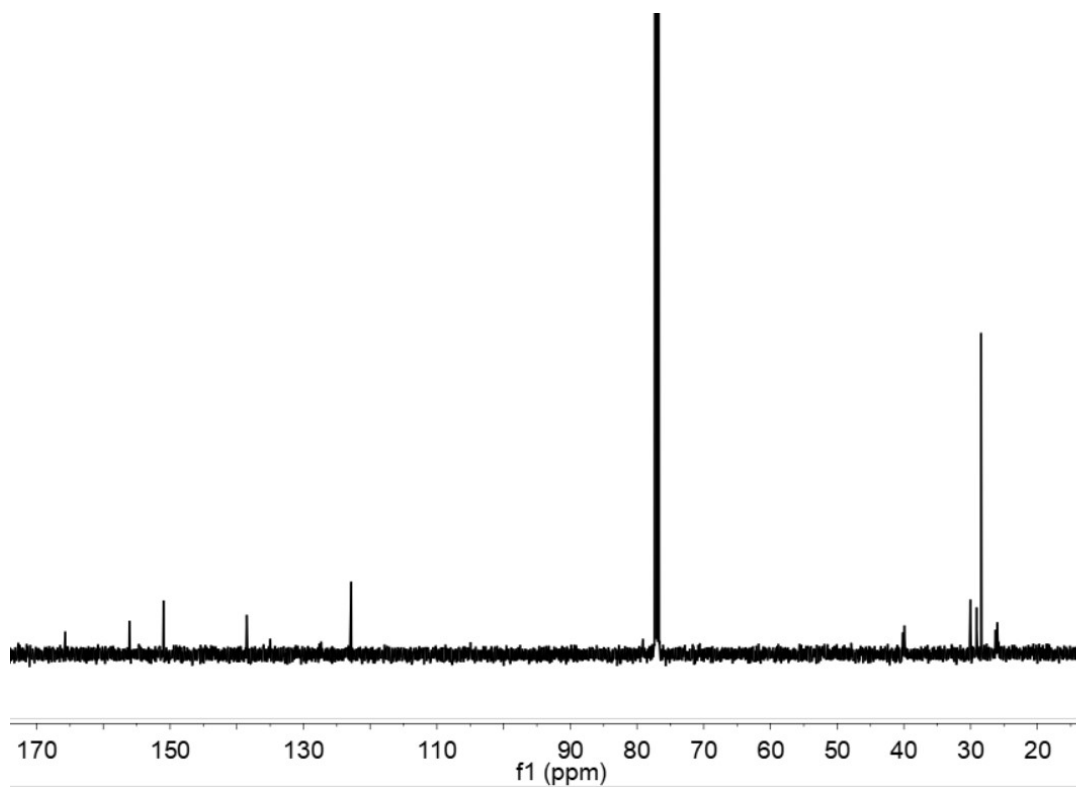


Figure S24. ¹³C NMR spectrum of **1-1** in CDCl₃.

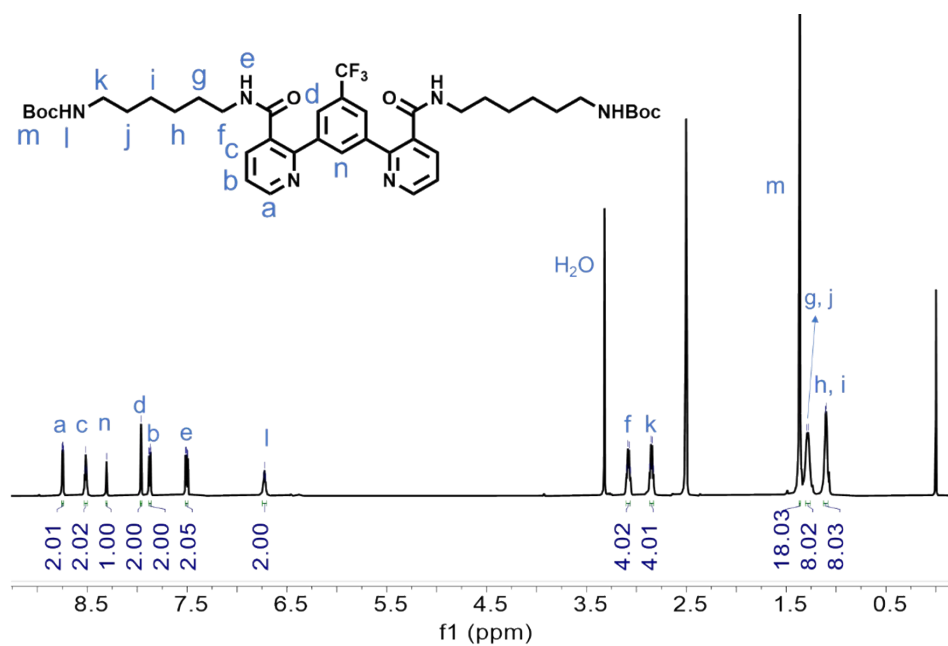


Figure S25. ^1H NMR spectrum of 1-3 in $\text{DMSO-}d_6$.

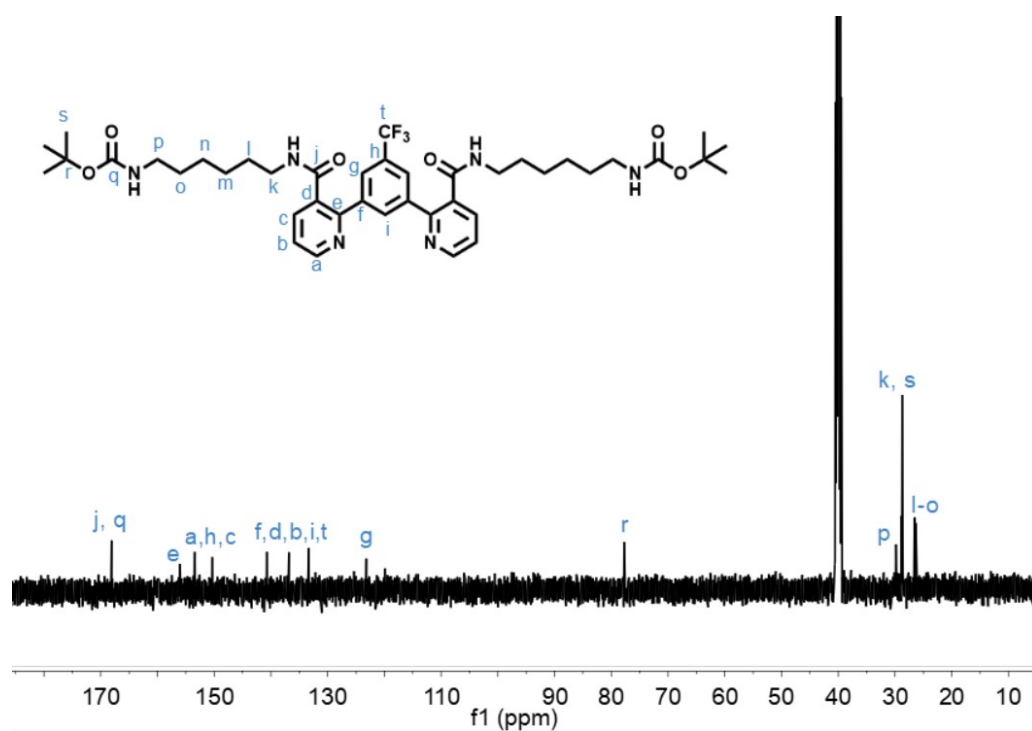


Figure S26. ^{13}C NMR spectrum of 1-3 in $\text{DMSO-}d_6$.

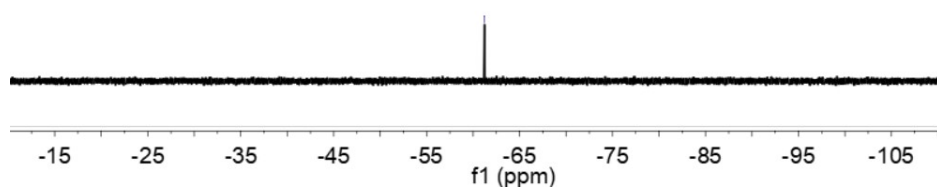


Figure S27. ^{19}F NMR spectrum of **1-3** in $\text{DMSO-}d_6$.

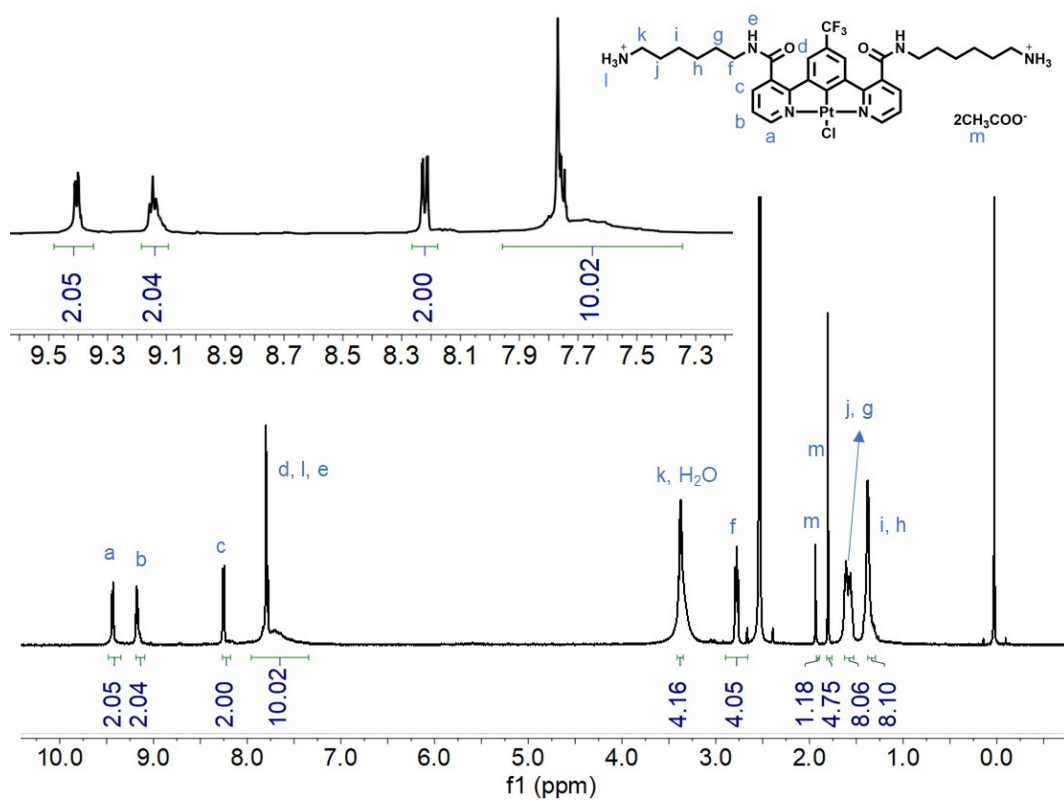


Figure S28. ^1H NMR spectrum of **1** in $\text{DMSO-}d_6$.

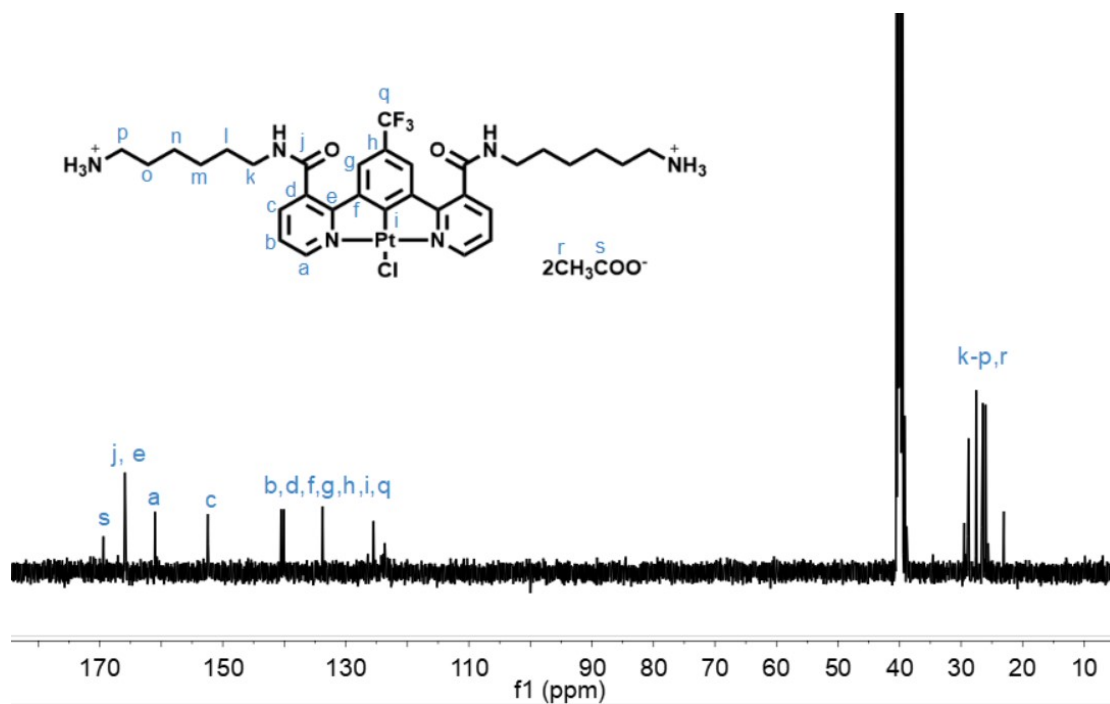


Figure S29. ¹³C NMR spectrum of **1** in DMSO-*d*₆.

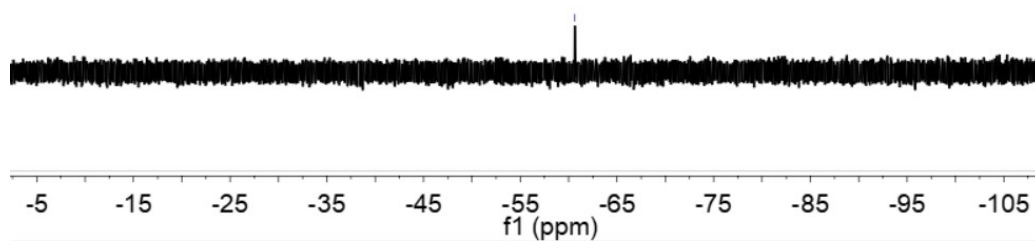


Figure S30. ¹⁹F NMR spectrum of **1** in DMSO-*d*₆.

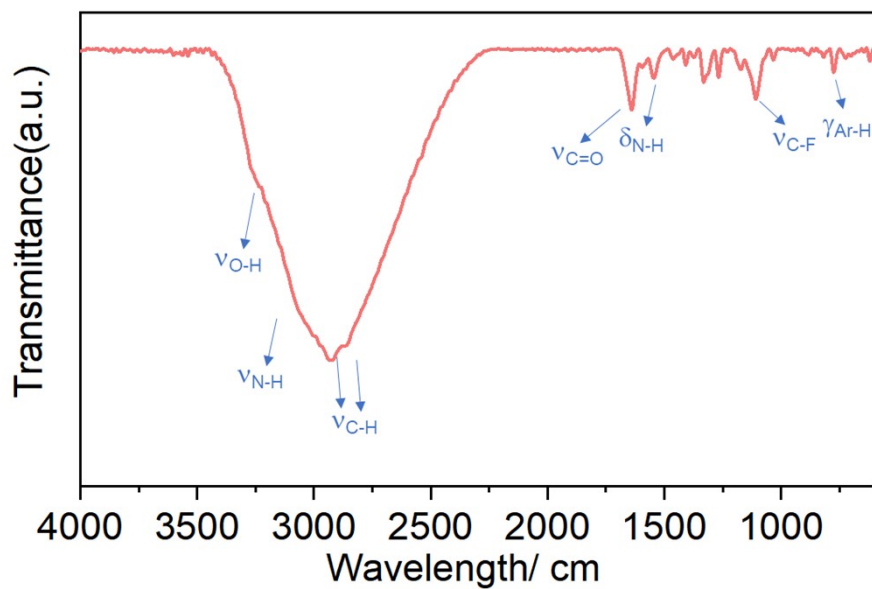


Figure S31. Infrared spectrum of **1**.

4. References

- [1] A.M. Mfuh, V.T. Nguyen, B. Chhetri, J.E. Burch, J.D. Doyle, V.N. Nesterov, H.D. Arman, O.V. Larionov, Additive- and metal-free, predictably 1,2- and 1,3-regioselective, photoinduced dual C–H/C–X borylation of haloarenes. *J. Am. Chem. Soc.* 138 (2016) 8408-8411.